

Image Processing for Workability of Concrete with Super Absorbent Polymer

Asgar Aryanfar¹✉ and Irem Şanal²

¹ American University of Beirut, RiadEl-Solh 1107 2020, Lebanon
 aryanfar@caltech.edu

² Bahçeşehir University, 4 Çırağan Cad, 34353 Istanbul, Beşiktaş, Turkey

Abstract. Super absorbent polymers (SAP) are the recent promising chemical admixtures with the potential for reducing the shrinkage, cracking, freeze/thaw and increasing the durability of the concrete [1–4]. These polymers are classified as hydrogels when cross linked and can retain exceptionally high amount of liquid solutions of their own weight [5]. In this paper, the flowability of the SAP is addressed by exploring the transient behavior in the viscoelastic properties of the SAP-contained concrete. Controlling flow within such relatively short period of time is essential for concrete functionality in construction.

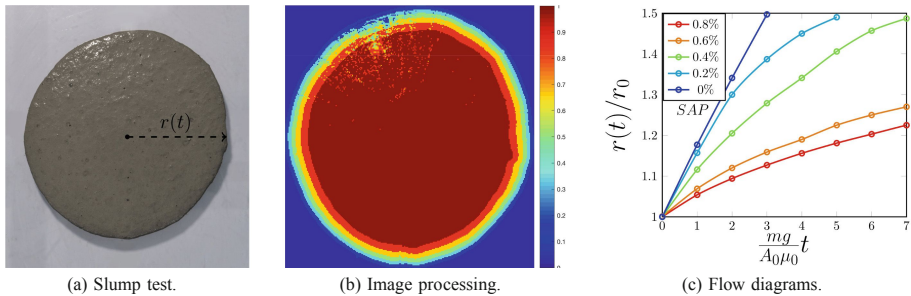


Fig. 1. Analysis.

1 Introduction

Super absorbent polymers have opened up new possibilities for controlling the control of free water in the concrete mixture, which controls both fresh and hardened state concrete properties through internal curing [6]. Such utilization as a self-curing agent saves water as the concrete dries to a large extent. Typical chemical composition is sodium salt of poly-acrylate acid $[-CH_2-CH(CO_2Na)-]_n$, a crystal-like structure classified hydrogel when cross-linked. They have capacity to take up and retain up to $\times 1000$ times their own weight. SAPs are commonly used in diapers, sanitary napkins, biomedical purposes, agriculture etc.

The recent introduction of SAPs into concrete has led to promising results in terms of physical and mechanical properties of the mortar as well as reliability in both fresh and hardened states. During absorption, water is entrained and cured into the concrete leading to hydration. Subsequently, SAP particles can slowly release their inner water as humidity supply when decreased in cement paste. This process fills the pores and reduces the micro-cracks, relieving the autogenous and drying shrinkages. Consequently the strength and durability of the concrete is enhanced [7]. Therefore, the release process of water as well as its magnitude is a critical parameter for investigation of internal curing.

Predicting and controlling the workability of SAP modified concretes during the mixing process is a limiting factor for the practical uses of these promising materials in concrete industry. Therefore, the main objective in this study is to propose an image based analysis for predicting SAP concrete's workability before casting process. For this purpose we characterize the transient behavior of cementitious composite modified with SAP in fresh state where we explore the radial propagation of slump and correlate the growth to the transient viscosity $\mu(t)$. Such depiction allows to predict and control the workability during concrete casting.

2 Methodology

2.1 Materials and Design

A simple test on mixing the water with the super absorbent powder shows that it can absorb up to 100g of water per gram of SAP as shown in the Fig. 2.

During mixing, the SAP particles increase in volume, which is similar to air entrainment technique, utilized for improving the resistance of concrete to freeze-thaw. The entrainment is homogenous and improves hardening of concrete [8].

The control mixture with the water-to-cement ratio of $w/c = 0.4$ was prepared as reference. The next mixtures contained varying amounts of $\{0.2\%, 0.4\%, 0.8\%\}$ in SAP of the cement mass. Additional water was added

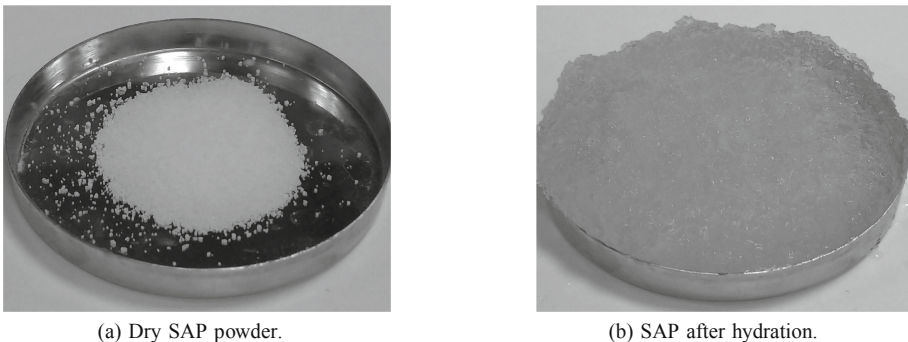


Fig. 2. Water absorption by SAP.

Table 1. Properties of SAP samples used.

$\rho(kg/m^3)$	$d_{particle}(\mu m)$	Absorption (g/g)	Desorption (%)	SAP content	SP content
1310	150 – 200	100	5	{0.2%, 0.4%, 0.8%}	{1%, 2%}

to compensate for the absorption of mixing water by the polymers and to create mixtures showing a similar workability to the reference with a water-to-cement ratio of 0.40. Consequently, polycarboxylate based superplasticizer was used to attain a self-compacting behaviour of the concrete, with the amounts of {1%, 2%}. A maximum aggregate size of 2mm for the fine aggregates of ordinary Portland cement with the grade *CEM*|42.5. The mortar samples were prepared in the room with temperature of $20 \pm 2^\circ C$, by mixing the solid powder with liquid for 2 min at low speed of $140 \pm 5 rev/min$ and a further 2 min at high speed of $285 \pm 10 rev/min$. The SAPs was treated by sieves, and the SAP with particle size of 150 – 200 μm was selected. The detailed properties of SAP used in this study is given in Table 1.

The mini slump flow was carried out by placing the cone in the middle of a flat piece of square glass and filled with mortar. The cone is then quickly lifted, allow the mortar to flow. After certain enlargement the sample turns to steady shape.

High resolution digital images (15 frames/second) were also taken at regular time intervals during the mini slump flow test to evaluate the flow behavior of materials in the subsequent computations.

2.2 Image Processing

The images from the bare concrete samples, given in Fig. 1a can be processed to get the area of the concrete in the given time $A(t)$ and the corresponding radius $r(t)$ respectively. The information from the red, green and blue values (i.e. $\{R, G, B\} \in [0, 255]$) can be transferred to a normalized gray-scale intensity image by averaging the values as:

$$I_{i,j} = \frac{R_{i,j} + G_{i,j} + B_{i,j}}{3 \times 255} \quad (1)$$

where the $I_{i,j} \in [0, 1]$ is the intensity value of the obtained grayscale image. The concrete regions can be distinguished by establishing a grayness threshold, $I_c \in [0, 1]$, which classifies the elements into black and white classes $\{B, W\} \in (0, 1)$. This value is determined iteratively from Otsu's method by minimizing the intra-class variance σ^2 as follows [9, 10]:

minimize σ^2 such that:

$$\begin{cases} \sigma^2 = \omega_1 \sigma_0^2 + \omega_2 \sigma_1^2 \\ \omega_1 + \omega_2 = 1 \end{cases} \quad (2)$$

where ω_1 and ω_2 are the fractions of black/white portions and σ_2^2 are the corresponding variances for each classified zone. The obtained binarized image provides the best approximation of the original gray-scale image since the minimization of intra-class variance σ^2 ensures the closest proximity in the values of each chosen group ($B\&W$) is chosen. Starting from the center, the cleared concrete area (ΔA_k) in each time t_k can be obtained by propagating through the first-order neighbors until no further progress is made [11]. Figure 1b represents the computed effective incremental area in the time-span of the experiment. Consequently, we define the measure of flowability F as the normalized radius ($F := \frac{r(t)}{r_0}$) which is tracked versus time. Figure 1c represents the computed measure for 4 concrete samples varying concentration in SAP.

The obtained values for the radius $r(t)$ can be differentiated to get the values of the radial velocity ($u_{k+1} = \frac{r_{k+1} - r_k}{\delta t}$). The flow is gravity-driven and the shear stress $\tau(t)$ versus shear rate ($\dot{\gamma} = du/dy$) would be related with viscosity $\mu(t)$ via Eq. 3:

$$\tau(t) = \mu(t) \frac{du}{dy} \tag{3}$$

On the other hand, we can simplify the Navier-Stokes relationship to describe the flow as [12]:

$$\frac{du}{dt} + u \frac{du}{dr} = \mu(t) \frac{d^2u}{dr^2} \tag{4}$$

The Eq. 4 can be solved using the finite-difference method. Using the scheme of forward in time and space ($FTFS$) for the experimental samples in the Fig. 1c, we get the value of the viscosity $\mu_k(t)$ as a function of SAP and SP contents, in the given time t_k as:

$$\mu_k = \left(\frac{u_{k+1} - u_k}{\delta t} + u_k \frac{u_{k+1} - u_k}{\delta r} \right) \left(\frac{u_{k+1} - 2u_k + u_{k-1}}{\delta r^2} \right)^{-1}$$

3 Results and Conclusion

The experimental and analytical results indicate that the proposed image based analysis technique has a potential to be used for automatic and practical estimate of SAP included concrete’s workability before casting process. The computations reveal that the viscosity $\mu(t)$ is significantly higher in the presence of augmented SAP mixture ($SAP \uparrow \sim \mu \uparrow$). This correlation however is opposite for the content of SP ($SP \uparrow \sim \mu \downarrow$). Such trade-off shows that combined utilization of SAP and SP contents can be used as determining parameters to tune the flow parameters to tune and control the workability properties of the concrete effectively.

References

1. Lee, H.X.D., Wong, H.S., Buenfeld, N.R.: Self-sealing of cracks in concrete using superabsorbent polymers. *Cem. Concr. Res.* **79**, 194–208 (2016)
2. Schröfl, C., Mechtcherine, V., Gorges, M.: Relation between the molecular structure and the efficiency of superabsorbent polymers (SAP) as concrete admixture to mitigate autogenous shrinkage. *Cem. Concr. Res.* **42**(6), 865–873 (2012)
3. Justs, J., Wyrzykowski, M., Bajare, D., Lura, P.: Internal curing by superabsorbent polymers in ultra-high performance concrete. *Cem. Concr. Res.* **76**, 82–90 (2015)
4. Mechtcherine, V., Reinhardt, H.-W.: Application of Super Absorbent Polymers (SAP) in Concrete Construction: State-of-the-art Report Prepared by Technical Committee 225-SAP, vol. 2. Springer Science & Business Media, New York (2012)
5. Esteves, L.P.: Superabsorbent polymers: on their interaction with water and pore fluid. *Cem. Concr. Compos.* **33**(7), 717–724 (2011)
6. Jensen, O.M.: Use of superabsorbent polymers in concrete. *Concr. Int.* **35**(1), 48–52 (2013)
7. Jensen, O.M., Hansen, P.F.: Water-entrained cement-based materials: I. principles and theoretical background. *Cem. Concr. Res.* **31**(4), 647–654 (2001)
8. Jensen, O.M., Hansen, P.F.: Water-entrained cement-based materials: II. experimental observations. *Cem. Concr. Res.* **32**(6), 973–978 (2002)
9. Otsu, N.: A threshold selection method from gray-level histograms. *Automatica* **11**(285–296), 23–27 (1975)
10. Aryanfar, A., Hoffmann, M.R., Goddard III, W.A.: Finite-pulse waves for efficient suppression of evolving mesoscale dendrites in rechargeable batteries. *Phys. Rev. E* **100**(4), 042801 (2019)
11. Aryanfar, A., Goddard III, W., Marian, J.: Constriction percolation model for coupled diffusion-reaction corrosion of zirconium in pwr. *Corros. Sci.* **158**, 108058 (2019)
12. Munson, B.R., Okiishi, T.H., Huebsch, W.W.: *Fluid Mechanics*. Wiley, Singapore (2013)